Oct 19th, 12:00 AM

Flexural Behavior of Profiled Composite Beams

Jun-Yep Song

Young Bong Kwon

Fifteenth International Specialty Conference on Cold-Formed Steel Structures
St. Louis, Missouri U.S.A., October 19-20, 2000

Flexural Behavior of Profiled Composite Beams

Jun-Yeup Song[1] and Young-Bong Kwon[2]

ABSTRACT

The behavior of composite beams, which are composed of cold-formed steel sheeting and normal strength concrete, has been studied. A series of flexural tests of composite beams has been executed and analytical methods to trace the nonlinear behavior of composite beams have been developed. The nonlinear moment-curvature relation of the composite beam has been described using a simple power model and cross section analysis procedure. The load-deflection behavior of the composite beam simulated by the step-by-step numerical integration method has been compared with test results.

1. INTRODUCTION

Cold-formed profiled steel sheeting has been widely used in the construction of composite slabs and used as a permanent formwork for non-composite slabs. The term permanent formwork indicates that the sheeting has not been removed after the hardening of the concrete material. The advantages of using profiled sheeting for composite slab construction included high degree of strength, ductility and material savings cost. Recent research has proven that the same advantages could be obtained in using profiled sheeting for composite beams. The profiled composite beam, which a reinforced concrete beam wrapped by the cold-formed profiled steel sheeting, might result in reduced span to depth ratio from increased strength and stiffness. The bond stress between steel and concrete, material strengths and thickness of steel section affect the strength and stiffness of composite beams. The ductility is mainly affected by the steel ratio and the shape of the steel section.

A straightforward method to predict the ultimate strength and moment-curvature relation of profiled composite beams, using the nonlinear stress-strain relations of both concrete and steel, has been studied by Uy and Bradford. Yang et al. described the moment-curvature relation in a simple power model, which could be used to trace the nonlinear load-deformation behavior of composite beams.

In this paper, the behavior of composite beams is investigated experimentally and compared with reinforced concrete beams, which have the same flexural strength or geometric dimensions respectively. The simple power model modified by the authors for the applications to the profiled cold-formed composite beams are calibrated by the test results. The beam-deflection curve method using above formulae and the step-by-step numerical integration procedures has been developed to trace the nonlinear load-deflection curve of composite beams

[1] Lecturer, School of Civil Engineering, Yeungnam University. Taegu, Korea
[2] Professor, School of Civil Engineering, Yeungnam University. Taegu, Korea

2 TEST SECTIONS

2.1 Geometry and Labeling

The composite sections tested were formed from a cold-reduced zinc-coated steel conforming to KS(Korean Standard) with a specified minimum yield strength of 240MPa. Two kinds of reinforcement steel bar were used in tensile and compressive zone with a minimum yield strength of 300MPa and 400MPa respectively. The important parameters considered for the composite sections are steel thickness and the shape of rib. The thickness of 1.2mm and 1.6mm was chosen to investigate the effects of the thickness on the flexural strength of the composite beam and two types of rib were selected to study the difference in bond and flexural strength. The type of concrete used was normal strength concrete.

The test sections were composed of real size beams and half size models to investigate the increase of ductility and flexural strength compared with the reinforced concrete beam. The sections have been designed that the real size composite beam has the same flexural strength as the reinforced concrete beam to be compared with and the half size model has the similar geometrical dimensions to the reinforced concrete beam. The geometry of the test sections is shown on Fig. 1(a) and (b) and Table 1(a) and (b).

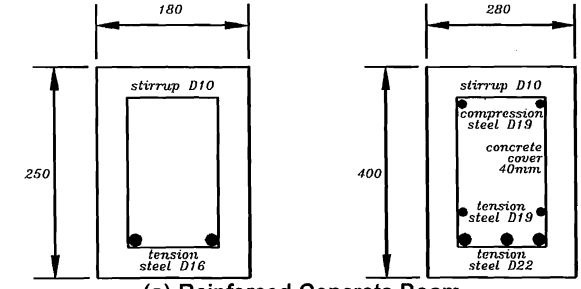

(a) Reinforced Concrete Beam

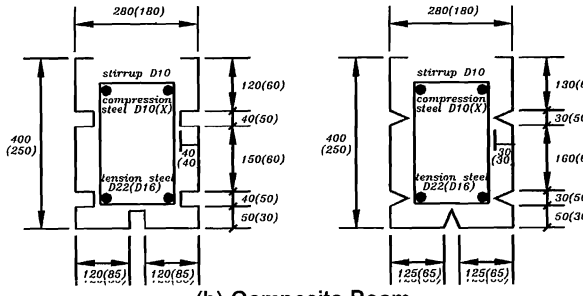

(b) Composite Beam

Fig. 1 Test Sections (unit : mm)

The test sections were labeled to indicate section size, rib shape, and thickness. In Table

1(a) and 1(b), specimen designations starting with R refer to reinforced concrete beams, and those starting with A and B refer to composite beams which thickness of profiled steel sheeting 1.2mm and 1.6mm respectively. The second character R and T indicate rectangular and triangular rib, and the third character, W or O, represents with shear stirrup and without shear stirrup, respectively. The numerals, 1 refers to the real size and 2 refer to the half size model section.

Table 1(a) Reinforced Concrete Beam Sections

Test Specimens	σ_{ck} (Mpa)	Cross section area (cm^2)	Reinforcing steel area (cm^2)	Reinforcing steel ratio	Length (cm)	Shear stirrup
R-RW-1	25.0	28×40	17.34	0.01874	450	Yes
R-RW-2	25.2	18×25	3.97	0.01103	200	Yes
R-RO-1	25.3	28×40	17.34	0.01874	450	no

Table 1(b) Composite Beam Sections

Test Specimens	σ_{ck} (MPa)	Cross section area (cm^2)	A_r (cm^2)	A_s (cm^2)	A_c (cm^2)	Reinforcing steel ratio	Length (cm)	Connecting
A-RW-1	25.0	28×40	7.74	17.7	1029.4	0.00892	450	Screw fastener
B-RW-1	25.0	28×40	7.74	23.7	1029.4	0.00892	450	Welding
A-TW-1	25.0	28×40	7.74	15.9	1073.3	0.00852	450	Welding
B-TW-1	25.0	28×40	7.74	21.2	1073.3	0.00852	450	Welding
A-RW-2	25.2	18×25	3.97	13.9	347.6	0.01329	220	-
B-RW-2	25.2	18×25	3.97	18.6	347.6	0.01329	220	-
A-TW-2	25.2	18×25	3.97	10.6	408.3	0.01127	220	-
B-TW-2	25.2	18×25	3.97	14.0	408.3	0.01127	220	-
A-RO-1	25.3	28×40	7.74	17.7	1029.4	0.00892	450	Screw fastener
A-TO-1	25.3	28×40	7.74	15.9	1073.3	0.00852	450	Screw fastener
B-RO-1	25.3	28×40	7.74	23.7	1029.4	0.00892	450	Screw fastener
B-TO-1	25.3	28×40	7.74	21.2	1073.3	0.00852	450	Screw fastener

2.2 Mechanical Properties

Cold-Formed Steel Sheeting And Reinforcing Steel Bar

The stress-strain relations of cold-formed steel sections generally shows gradual yielding since non-uniform plastic deformation of the cross section caused differences in the yield strength and residual stress of the fiber. The test yield strength of the section is generally higher than the nominal strength and the strength variation of the corner area is greater than that of the flat area. However, regardless of the position, the nonlinear stress-strain relations of profiled steel sheeting can be formulated by the Ramberg-Osgood formula as Eq. (1).

$$\varepsilon = \frac{\sigma}{E} + \varepsilon_p \left(\frac{\sigma}{\sigma_p}\right)^n \quad (1)$$

The stress-strain relation is shown on Fig. 2 and the mechanical properties of the cold-formed steel section are given in Table 2.

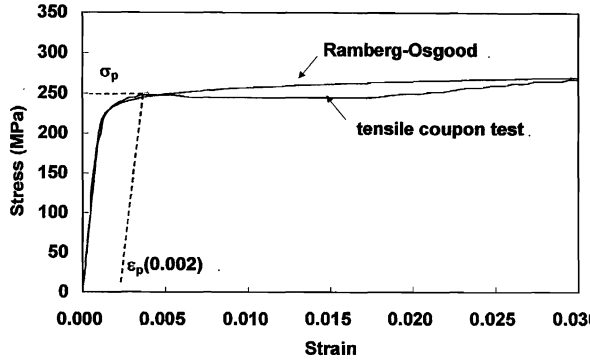

Fig. 2 Stress-Strain Curve of Cold-Formed Steel Sheeting

Table 2 Mechanical Properties of Tensile Coupon

Specimen	Thickness (mm)	E_s (MPa)	σ_y (MPa)	σ_u (MPa)	ε_u
Plate	1.2	207000	260.0	344.8	0.159625
	1.6	209000	250.0	333.3	0.162125

The stress-strain relation of reinforcing steel bars has been assumed to be bilinear. The curve shows that an inclined straight line with Young's Modulus up to the yield stress and then a horizontal line take place, while neglecting the strain-hardening range of the properties. The mechanical properties of reinforcement bar are given in Table 3. The yield and ultimate tensile stress are slightly higher than the nominal strength of 300Mpa and 400MPa

Table 3 Mechanical Properties of Reinforcing Steel Bar

Reinforcing steel	Grade	Yield stress (MPa)	Ultimate tensile stress (MPa)	Cross section area (cm^2)
D10	SD30	350	510	0.713
	SD40	440	630	
D16	SD30	350	600	1.986
D19	SD40	440	620	2.865
D22	SD40	420	610	3.871

Concrete

The stress-strain relation proposed by Hognestad was used for the numerical model.

$$\sigma = (0.85 \times \sigma_{ck}) \left[\frac{2\varepsilon}{\varepsilon_0} - \left(\frac{\varepsilon}{\varepsilon_0} \right)^2 \right] \tag{2}$$

where, $\varepsilon_0 = \dfrac{2 \times (0.85\sigma_{ck})}{E_c}$

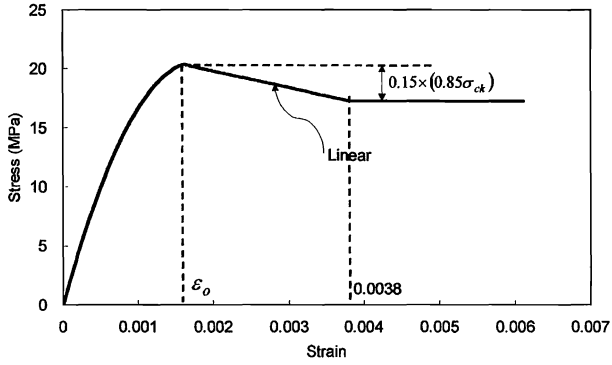

Fig. 3 Compressive Stress-Strain Relation of Concrete

The concrete tensile strength and strain relation proposed by Lin and Scordelis, as a function of compressive strength, is chosen to include the tensile strength of the tension area of the composite beam section and expressed as Eq. (3a-b).

$$0 \le \varepsilon \le \varepsilon_{cr} \quad \sigma = E_c \times \varepsilon \tag{3a}$$

$$\varepsilon \ge \varepsilon_{cr} \quad \sigma = \sigma_{cr} \times \left(\frac{\varepsilon}{\varepsilon_{cr}} \right)^c \tag{3b}$$

where, $\sigma_{cr} = 2.0\sqrt{\sigma_{ck}}$, ε_{cr} = strain at the moment that the initiation of crack, $c = -0.4$

The average values of concrete compressive strength obtained from five cylinders cast from the same batch of the reinforced concrete beams are given in Table 4.

Table 4 Concrete Cube Test Results

No.	Batch 1 (MPa)	Batch 2 (MPa)	Batch 3 (MPa)
Average	25.0	25.3	25.2

3. FLEXURAL TESTS

3.1 Test Arrangements

The sections were tested to failure in flexure using a third-point loading that produces a constant moment region for a simply supported beam. Since test series 1 sections were 4500mm in length, the test setup was composed with a hydraulic jack and strong frame instead of Universal Testing Machine (capacity of 1000MPa) which was used for test series 2 sections. Two LVDTs were placed at the third point and one at midspan to monitor the load-deflection characteristics. The test setup is shown Fig. 4. Strains were measured at midspan throughout the depth of the cross section and reinforcing steel using strain gauges for concrete and steel. The strain gauge locations are shown on Fig. 5. These measured strains were used to determine the curvatures and slip strains of the composite beam.

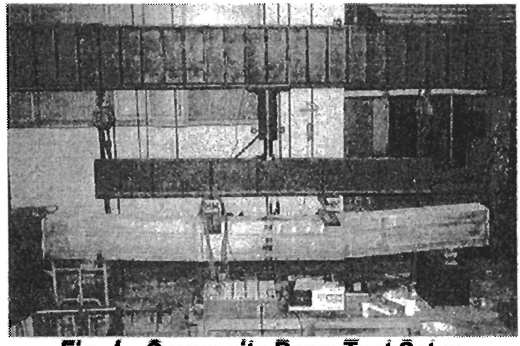

Fig. 4 Composite Beam Test Setup

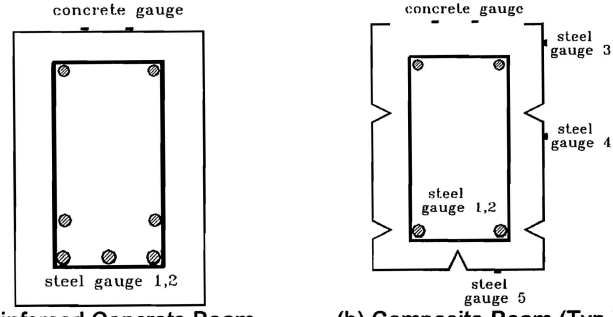

(a) Reinforced Concrete Beam (b) Composite Beam (Typ.)

Fig. 5 Strain Gauge Location

3.2 Flexural Test Results

The ultimate moment M_u, nominal moment M_n calculated according to the ACI

specifications and plastic moment M_{pc} determined by Eq.(4a) and the moment M_t calculated using the cross section analysis procedure of reinforcement and composite beams are given on the Table 5.

Table 5 Flexural Strength of Test Sections

Test specimen	M_u (kN-m)	M_n (kN-m)	M_{pc} (kN-m)	M_t (kN-m)	M_u/M_n	M_u/M_{pc}	M_u/M_t
R-RW-1	220.5	190.4	-	200.3	1.15	-	1.10
R-RW-2	28.2	24.2	-	25.6	1.16	-	1.10
A-RW-1	143.2	104.3	181.3	190.7	1.37	0.79	0.75
B-RW-1	190.5	104.3	201.7	212.2	1.83	0.94	0.90
A-TW-1	177.8	105.3	178.4	171.1	1.69	0.99	1.03
B-TW-1	188.8	105.3	197.3	188.7	1.97	0.96	1.00
A-RW-2	60.9	23.4	61.9	61.4	2.60	0.98	0.99
B-RW-2	63.8	23.4	64.8	65.8	2.72	0.98	0.97
A-TW-2	50.8	23.7	53.8	49.9	2.14	0.94	1.01
B-TW-2	51.9	23.7	60.9	56.1	2.19	0.95	0.92

The plastic moment can be obtained by assumption of full plastic state of the material, which is shown on Fig. 6.

$$M_{pc} = t_e d_n^2 \sigma_y + \frac{1}{2} k_1 d_n^2 (B_e - 2t_e)\sigma_{ck} + 2B_r t_e (d_n - \frac{t_e}{2})\sigma_y$$
$$+ \frac{2\pi d_c^2}{4}(d_n - c_c - \frac{d_c}{2})\sigma_{b,y} + t_e (D - d_n)^2 \sigma_y \qquad (4a)$$
$$+ t_e (B_e - 2t_e)(D - d_n - \frac{t_e}{2})\sigma_y + \frac{2\pi d_t^2}{4}(D - d_n - c_t - \frac{d_t}{2})\sigma_{b,y}$$

where,

$$d_n = \frac{t_e(2D + B_e - 2t_e - 2B_r)\sigma_y + \frac{\pi}{4}(2d_t^2 - 2d_c^2)\sigma_{b,y}}{4t_e\sigma_y + k_1(B_e - 2t_e)\sigma_{ck}} \qquad (4b)$$

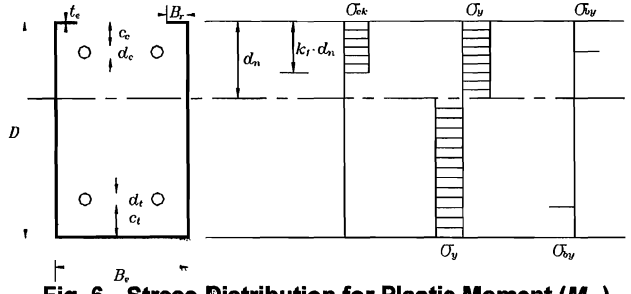

Fig. 6 Stress Distribution for Plastic Moment (M_{pc})

The failure load of the cold-formed steel thickness t=1.6mm is higher than that of the section of t=1.2mm by 10-20%, rectangular rib section is stiffer than triangular rib by approximately 15-30%. The continuous fillet weld combined with fastener connection seems to be reasonable connecting method in large size sections. The stiffening effect is very clear since the failure moment approaches 95% of the ultimate moment. The flexural moment of the composite sections was increased by 1.5 to 2.5 times in comparison with the same size reinforced concrete beams.

Rectangular rib can be regarded as a better shape than triangular one since the flexural moment is increased slightly due to the increase of steel cross section and contact area between steel and concrete. The bond strength of rectangular rib is also higher than the triangular one. However, the ductility is slightly decreased due to the increment of reinforcement steel ratio. The nominal moment M_n obtained using transformed equivalent concrete section with elastic modulus ratio of steel and concrete cannot be acceptable since the interaction between steel and concrete and the stress-strain relation beyond elastic range cannot be included in that way. The method underestimates the flexural strength of the composite section. The plastic moments which is generally used in the strength design method, produces reasonable values except A-RW-1 and B-TW-2. The ultimate moment determined by the cross section analysis is exactly the same as the plastic moment.

The loads versus strain curves are shown on Fig. 7. The stress-strain curves of reinforcing bar and steel section have shown typical relation respectively. However the load-strain relation of concrete was different from that of the compressive stress-strain relation. The load-strain curve of reinforcing bar showed bi-linear relation. The strain of the reinforcing steel was increased slowly as the load was increased up to approximately 0.002 where it yielded. The cold-formed steel sheeting of bottom flange yielded gradually with increase of loading. An increase in ductility after the maximum strength was shown due to the interaction between concrete and steel. The concrete top fiber strain was increased nonlinearly up to the strain of 0.002 and the ultimate strain at failure was over 0.003 which meant that the failure of concrete was delayed by the confining effect of the steel section.

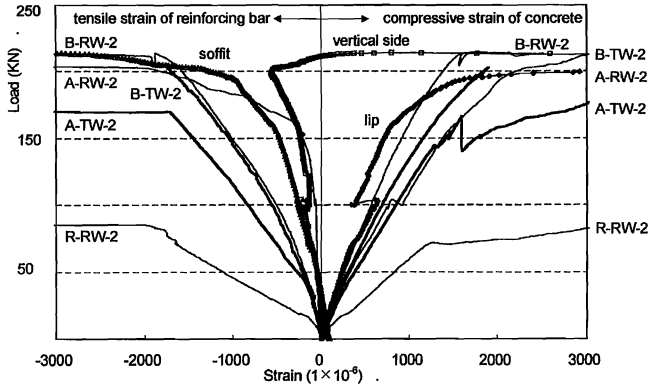

Fig. 7 Load versus Strain Curve

3.3 Shear Strength of Composite Beams

The nominal shear strength and the maximum shear force at failure of the reinforced concrete section and the composite section are shown on the Table 6 in order to investigate the necessity of the shear stirrup against shear force. The maximum shear force was measured at failure of beams and the nominal shear strength was determined according to ACI. The shape and growth of shear cracks of composite sections cannot be observed due to the wrappage of steel. The steel section was uncovered to investigate the crack. However, shear cracks were not found even for the composite section without stirrup. The shear strength of steel sections is taken as Eq. (5a) and the ratio of sharing shear stress to ultimate shear strength of the steel section is expressed as Eq. (5b).

$$V_s = \tau_y \cdot A_w = 0.6\sigma_y A_w \tag{5a}$$

$$\frac{\tau_s'}{\tau_y} = \frac{V_s'}{V_s} = \frac{V_s'}{A_w \tau_y} \tag{5b}$$

where A_w is the web area of steel sections.

Table 6 Shear Strength of Composite Sections

Test specimen	V_u (kN)	V_n (kN)	V_c (kN)	V_s (kN)	V_r (kN)	V_s' (kN)	$\frac{\tau_s'}{\tau_y}$	$\frac{V_u}{V_n}$	$\frac{V_u}{V_c+V_s}$
R-RO-1	112.0	93.0	93.0	-	-	-	-	1.2	-
A-RO-1	128.8	218.0	76.1	141.9	111.0	52.7	0.37	0.59	0.59
A-RW-1	147.4	329.0	76.1	141.9	111.0	71.7	0.51	0.44	0.68
A-TW-1	177.8	332.0	79.6	141.4	111.0	98.2	0.69	0.54	0.80
B-RW-1	192.3	369.0	76.1	181.9	111.0	116.2	0.64	0.52	0.75
B-TW-1	188.6	372.0	79.6	181.4	111.0	109.0	0.60	0.51	0.72

Since moment failure occurred for the sections with shear stirrup rather than shear failure, the comparison between nominal and ultimate shear strength of the section is not possible. However, the difference in shear strength of A-RW-1 and A-RO-1 means the stirrup increase shear strength slightly at the failure load. The nominal shear strength composed of the shear strength of steel sheeting and concrete is enough to resist against the maximum shear force. The ratio of maximum shear strength to nominal shear strength is ranged from 0.44 to 0.59 for the sections with stirrup. Consequently, the shear stirrup reinforcement of the composite section need not be placed for general shallow beams, which may have moment failure.

4. MOMENT-CURVATURE RELATIONS OF COMPOSITE BEAMS

A couple of numerical procedures proposed by yang et al. for the moment-curvature relation of composite beams based on the cross section analysis and a simple power model are briefly explained proposed and compared with the experimental results.

4.1 Cross Section Analysis

The cross section analysis procedure is adopted and modified from what was developed by Uy and Bradford. The entire cross section of the composite beam is divided into thin horizontal layers. The strain distribution is assumed to be linear. The stress at each layer can be calculated with the stress-strain relation of cold-formed steel, reinforcing steel bar, and concrete respectively. The axial force and the bending moment of all layers are summed up. The bisection method is used to find the converged neutral axis depth for which the resultant axial force equals zero to a given accuracy. This procedure is iterated for the increased top strain of the section to obtain the moment-curvature relation.
The results obtained by the cross section analysis are given and compared with tests in Figs. 8(a) and (b). The comparison shows that the method produces quite reasonable moment-curvature relations.

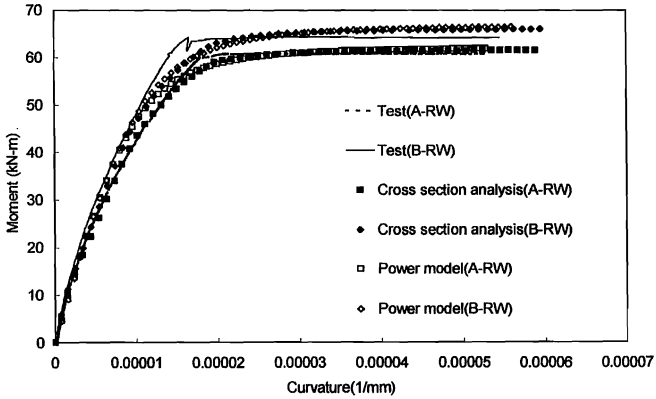

Fig. 8 (a) Moment-Curvature Relation for Rectangular Rib Beam

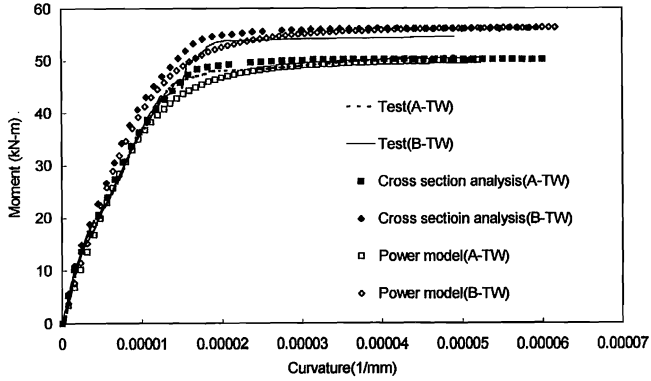

Fig. 8 (b) Moment-Curvature Relation for Triangular Rib Beam

4.2 Power Model

The second method to obtain the moment-curvature relation of the composite section is expressed in the function of simple power model, which is easily applicable, in order to obtain a comparatively accurate curve fit with less data. Kishi and Chen's power model, selected in this paper, needed initial connection stiffness, ultimate moment capacity and shape parameter.
The results obtained by the proposed Power Model are shown in Figs. 8(a) and (b), where the shape parameter shape parameter was taken as 2.8. As shown on the figures, the model can produce a reasonable moment-curvature relation of the composite beam that is composed of cold-formed sheeting and concrete. The power model gives a slightly stiffer slope than the test results after local buckling occurred as in the cross section analysis. The local buckling of the steel plate, above top rib, cannot be included in this formula. However, the occurrence of local buckling of the steel plate does not affect the ultimate flexural rigidity of the composite sections, since the post-buckling stage is stable in the local buckling mode.

5. LOAD-DEFLECTION BEHAVIOR OF COMPOSITE BEAMS

The nonlinear load-deflection relation can be obtained simply by the numerical method, using the known moment-curvature relations. The step-by-step numerical integration method, with the previous moment-curvature relation model, is developed to trace the load-deflection relation of the profiled composite beam.
The results obtained by the moment-curvature relations which, is based on the Power Model, are shown and compared with the test results in Fig. 9(a) and (b). The comparison shows that the ultimate load is well agreed with the test results. However, the flexural stiffness is disagreeable, since the local buckling of the steel and the slip between steel and concrete cannot be properly included in the analysis of moment-curvature relations.

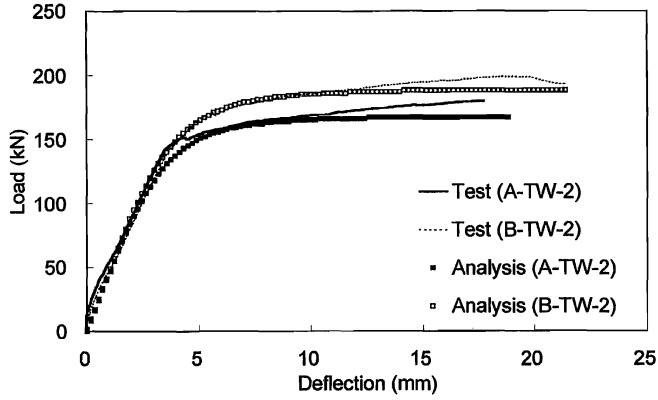

Fig. 9 (a) Load-Deflection Curve for Triangular Rib Section

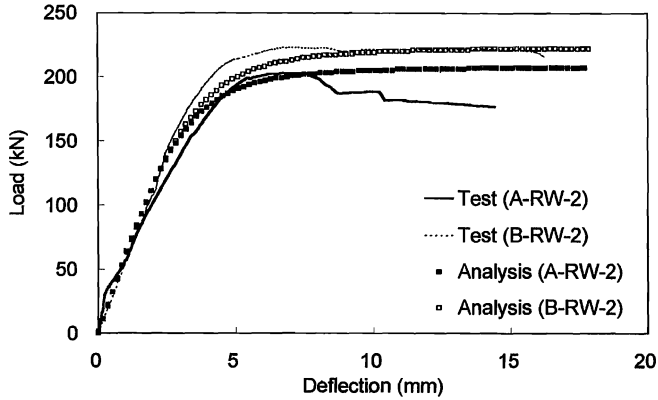

Fig. 9 (b) Load-Deflection Curve for Rectangular Rib Section

The neutral axis depth and ultimate flexural strength are given in Table 7 to investigate the effect of bond strength between steel and concrete on the flexural strength. The slip between steel and concrete is negligible for the section with rectangular rib but the slip of the section with triangular rib is approximately 7-8% of total strain. The difference between the test result and theoretical flexural strength for perfect composite sections is ranged from 2% to 15% due to slip between steel and concrete. The flexural strength of noncomposite section is lower than fully composite section by 18%. The neutral axis depth of steel concrete is quite similar, but significantly different for triangular rib section due to large amount of the slip. Consequently, the rectangular rib can be recommended rather than triangular rib.

Table 7 Flexural Strength for Composite and Noncomposite Beams

Test specimen	M_u (kN-m)	M_{pc} (kN-m)	M_{nsc} (kN-m)	N_c/D_e	N_p/D_e	M_u/M_{pc}
R-RW-2	28.2	24.2	-	-	-	1.16
A-RW-2	60.9	61.9	53.5	0.63	0.51	0.98
B-RW-2	64.4	64.8	55.2	0.61	0.50	0.98
A-TW-2	50.8	53.8	44.8	0.74	0.47	0.94
B-TW-2	51.9	60.9	50.3	0.34	0.81	0.85

6. CONCLUSION

A series of composite beam has been tested and analytically studied to investigate the flexural behavior. The flexural strength and stiffness of the composite beams were highly increased in comparison with the equivalent reinforced concrete beam. Though there is not much difference between rib types, the rectangular rib is better for bond strength than the triangular rib. The thickness of steel section has a significant effect on the flexural strength and stiffness as expected. The shear stirrup need not be added to resist against shear

force for the shallow beams.
A cross section analysis procedure and a simple Power Model to trace the nonlinear moment-curvature relation of the composite beam have produced reasonable agreement with test results. The step-by-step numerical integration method with the proposed moment-curvature models can simulate the load-deflection relation of the profiled composite beam and has been proven to be accurate and effective. However, the methods proposed need to be verified further by comparison with various test results.

REFERENCES

1. Chen W. F. and Lui E. M., *Structural Stability*, Elsevier Pty. Ltd. 1996.
2. Hognestad E., A study of combined bending and axial load in reinforced concrete members, University of Illinois Engineering experimental station, Bulletin series No. 399, (1951) pp.128.
3. Lin, A. M. and Scordelis, A. C., *Nonlinear Analysis of RC Shells of General Form*, *J. of Struct. Enging ASCE*, **101**(3) (19975) pp. 523-538.
4. Oehlers D. J., Wright H. D. and Burnet M. J., Flexural strength of profiled beams, *J. of Struct. Enging ASCE*, **120**(2), (1994) pp. 378-393.
5. Uy B. and Bradford M. A., Ductility and member behavior of profiled composite beams. Part : Experimental study, *J. of Struct. Enging ASCE*, **121**(5), (1995a) pp. 876-882.
6. Uy B. and Bradford M. A., Ductility and member behavior of profiled composite beams. Part : Analytical study, *J. of Struct. Enging ASCE*, **121**(5) (1995b) pp. 883-890.
7. Yang G. R., Hwang Y. S. and Kwon Y. B., A study on the flexural behavior of profiled composite beams. *The 14th International Specialty Conference on Cold-Formed Steel Structures*, St. Louis, MO (1998) pp. 393-406.

NOTATION

A_r : Reinforcing steel area
A_s : Profiled steel sheeting area
A_c : Concrete area
ε_p : Plastic component of the strain (usually 0.2%)
σ_p : Proof stress corresponding to 0.2% strain
n : Shape of the knee of the curve (n=25: for cold-formed steels)
σ_{ck} : Compressive strength of a concrete cube
V_u : Maximum shear force at failure
V_c : Shear strength of concrete
V_s : Shear strength of steel
V_r : Shear strength of stirrup
V_s' : V_u-V_c
V_n : V_s+V_c+V_r
M_{nsc} : Ultimate flexural strength for noncomposite section
D_e : Beam depth